A G-Band Glass Interposer Technology for the Integration of an Amplified Noise Source based on SiGe BiCMOS 55-nm Technology

Maya Alawar, Victor Fiorese, Sylvie Lépilliet, Daniel Gloria, Guillaume Ducournau, Emmanuel Dubois

A G-Band Glass Interposer Technology for the Integration of an Amplified Noise Source based on SiGe BiCMOS 55-nm Technology

Maya Alawar[#$], Victor Fiorese[*], Sylvie Lépilliet[#], Daniel Gloria[$], Guillaume Ducournau[#], Emmanuel Dubois[#]

[#]Univ. Lille, CNRS, Centrale Lille, Univ. Polytechnique Hauts de France, Junia, UMR 8520 – IEMN –Institut d'Electronique, de Microélectronique et de Nanotechnologie, France

[$]STMicroelectronics, QMT- Smart Power & Dig FEM-TDP Organization, France

[*]STMicroelectronics, MDG-RFC Organization, France

{maya.alawar.etu, emmanuel.dubois}@univ-lille.fr

***Abstract*— This paper introduces a substrate technology that integrates an amplified noise source (NS) based on SiGe BiCMOS B55 nm technology onto a glass interposer to reduce dielectric and transition losses. Previous work has focused on the development and characterization of the NS in two distinct configurations. In a first flavor, on-wafer noise measurements yielded to an extracted excess noise ratio (ENR_{av}) level of 37 dB in the 140-170 GHz. In an alternative approach, the NS was packaged in a split-block with a WR5.1 flange termination for connection to commercial passive probes, achieving an ENR_{av} level of up to 25 dB in G-band (140-220 GHz) corresponding to a 12 dB ENR reduction when compared to the on-wafer measurements. To reduce dielectric losses due to the substrate, this paper proposes a third integration route based on an ultra-thin glass interposer, AF32 from Schott. This solution implements femtosecond laser micro-machining to structure the interconnects, enabling the integration of the NS chip on the same substrate used to manufacture the coplanar probing tips, with the advantage of simplifying the signal propagation path. This work has achieved a tunable ENR_{av} level of up to 29 dB in the 140-170 GHz range, with constant output impedance matching better than -12 dB across the entire frequency band.**

***Keywords*— SiGe BiCMOS 55 nm, Noise Measurements, G-band, Packaging, Glass Interposer, Laser Micromachining.**

I. Introduction

III–V semiconductors have traditionally been the technology of choice for mmW applications, now largely challenged by the performance of advanced silicon technologies across the mmW and THz spectra [1], paving the way for cost-effective solutions that are required for mass market applications. Advanced silicon technologies which target f_T/f_{max} cut-off frequencies above 400 GHz, will enable the development of silicon circuits in the G-band. The validation of these technologies requires microwave characterization resources, in particular noise measurement, which is of utmost importance to extract transistor performance figures, including the noise figure (NF) and the four noise parameters (F_{min}, R_n, Y_{opt}). Among important issues for noise characterization in the G-band and beyond is the commercial availability of the noise source (NS) and the high sensitivity receiver [2].

Several studies have demonstrated the possibility of performing noise measurements in G-band, by integrating the broadband instrumentation electronics directly on the silicon around the device under test (DUT) using BiCMOS B55X technology [2,3], as it is described in Fig. 1a (the NS is off-wafer and the low noise amplifier (LNA)/tuner are monolithically co-integrated with the DUT). However, this approach of built-in-self-test (BIST) is not a viable solution, as it consumes a substantial amount of silicon surface area, resulting in unacceptable costs.

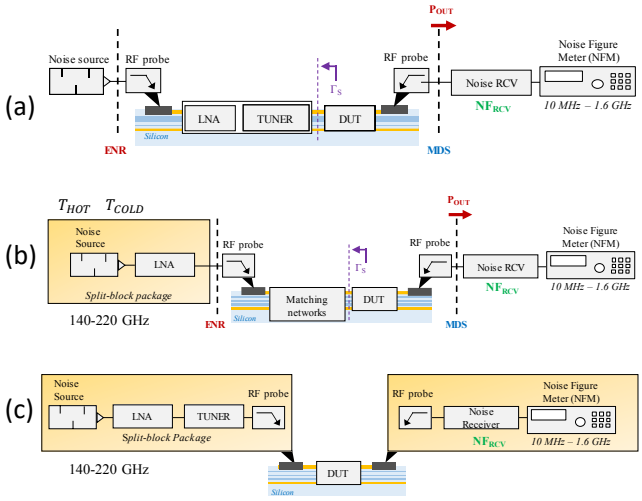

Fig. 1. Schematic representation: (a) built-in self-test [4]; (b) packaged active noise source ([4], [5], [6]); (c) integrated instrumentation system in the form of a functionalized active probe for the measurement of silicon components in the G-band. MDS = Minimum Detectable Signal.

Moreover, to use the instrumentation chain for a range of technologies beyond the B55X process and to rationalize the test costs, the main concept is to move from BIST to smart probes, where the integration of these functions in a compact system located as close as possible to the measurement tips must be developed (Fig. 1c). In this context, a SiGe BiCMOS technology-based packaged NS/LNA operating in G-band was presented for the first time in [6] (schematic diagram in Fig. 1b). When directly measured on-wafer, this NS generates a tunable excess noise ratio (ENR_{av}) level up to 37 dB in the 140-170 GHz range and up to 25 dB when the same NS is packaged in a split-block with WR5.1 flange termination. This results in an additional loss of 12 dB in the packaged configuration [7]. This paper proposes a new substrate technology to open up the possibility of integrating the NS on the same substrate used to manufacture the coplanar probing tips, with the advantage of

considerably simplifying the signal propagation path to feed the DUT at wafer level.

Section II recalls the state of the art with the split-block design and ENR_{av} extraction measurements of the amplified NS based on SiGe BiCMOS 55 nm technology for the packaged and on-wafer noise measurements. Section III details the design, fabrication, and assembly on a low-loss glass substrate which aims to mitigate losses observed in the packaged configuration. Section IV presents the main characterization results obtained in G-band in terms of S-parameters and ENR_{av}, along with a thorough description of the extraction methodology. Section V presents the measurement repeatability for S-parameters and ENR_{av} of three different assembled NS on the glass interposer. Finally, section VI provides the conclusion and prospects.

II. SiGe BiCMOS 55nm Amplified Noise Source

A. Description of the Packaged Noise Source Version

The substrate hosting the NS chip was a six metallic layer organic substrate stack compatible with routing both the RF signal and DC biases, as outlined in [7]. The NS was packaged in a split-block with a WR5.1 flange termination, allowing interconnection with standard external probes (Fig. 2). The transition of propagation mode from the organic substrate to the waveguide is achieved through an E-plane probe that was optimized for performance in G-band [8].

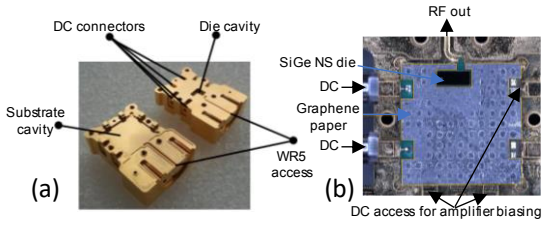

Fig. 2. (a) Machined split-block view, (b) opened split-block package after assembly and tightening of an organic substrate, showing the RF and DC bias access to the chip.

B. Excess Noise Ratio Extraction for on-wafer and packaged measurements

On-wafer noise measurements for the amplified NS revealed a maximum ENR_{av} level of about 37 dB at 170 GHz (Fig. 3a). This was followed by G-band measurements at the WR5.1 termination of the package output, resulting in ENR_{av} level up to 25 dB (Fig. 3b), thus highlighting a loss level of about 12 dB within the packaged configuration.

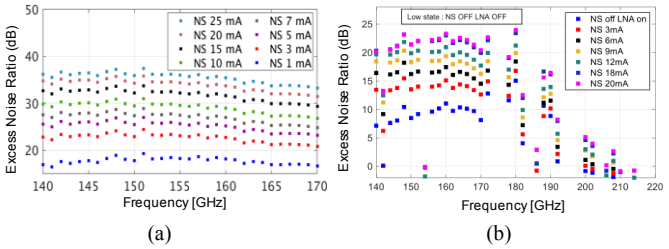

Fig. 3. Extracted ENR_{av} (dB) of the amplified NS: (a) on-wafer noise measurements within the 140-170 GHz frequency range (b) at the package output in G-band [6].

III. Integration of Amplified Noise Source on Glass Interposer

A. Design & Fabrication Concept

This section presents the design and fabrication of a glass interposer to avoid losses involved in the packaged noise source. This is accomplished by initially designing a 50 Ω grounded coplanar waveguide (GCPW) line with a transition to the pad for routing the RF signal to the chip. Femtosecond laser micromachining is used to pattern the chip interconnects (pad ring, CPW, and DC routing lines) on a 50 µm thick glass with a 1 µm gold overlayer. Fig. 4 shows an optical microscope observation of the machined interposer, achieved by controlling various laser process parameters, including average laser source power, pulse frequency, scan speed and beam width.

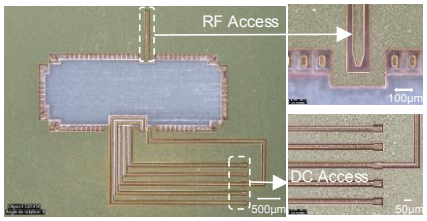

Fig. 4. Optical microscope observation of the machined interconnects of the interposer for routing DC and RF access to and from the chip, respectively.

B. Pick & Place Assembly

The assembly of the NS chip on the glass interposer is carried out using a semi-automatic pick-and-place equipment.

The interconnect structure applied to the NS chip consists of copper pillars covered by tin-silver (SnAg) balls with a melting temperature of 221°C [9]. This feature makes it possible to implement flip-chip thermocompression during assembly. However, and unlike a typical process, the upside of the NS chip is placed on the hot plate while the interposer is flipped, picked and placed over the chip, as depicted in Fig. 5(a) and Fig. 5(b). This unique approach, combined with the transparency of glass, enables the direct alignment using the same top camera. Following the bonding process, the assembly is examined through optical microscopy, as shown in Fig. 5(c).

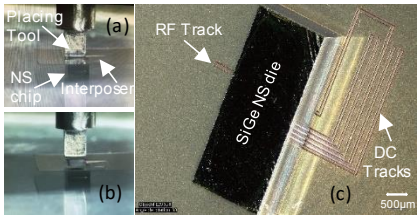

Fig. 5. Side camera pictures of the interposer and NS chip during assembly for place position (a) and tool removal (b), and an optical microscope observation of the assembled NS chip on glass interposer (c).

IV. Measurements of the Integrated Amplified NS on Glass Interposer

A. S-Parameter Measurements in G-Band

One-port S-parameters measurements were performed to characterize the NS chip assembled onto the glass interposer

with a Rohde & Schwarz vector network analyzer (VNA) with extension heads in G-band. The setup view proposed in Fig. 6b allows to characterize the output matching of the amplified NS for several bias conditions. In Fig. 6a, the S-parameters measurement of the amplified NS on the glass interposer shows a constant output matching better than -12 dB over the entire frequency range, offering a direct comparison with S_{22} of the NS measured both on-wafer and at the output of the packaged NS version. The observed shape in the S_{22} of the packaged NS at 190 GHz is attributed to the insertion loss (IL) of the substrate to waveguide transition.

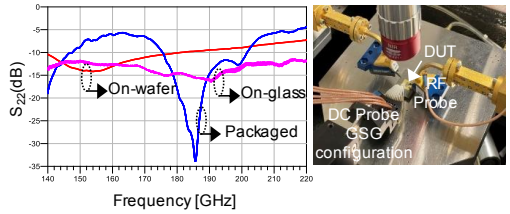

(a) (b)

Fig. 6.(a) Comparison of the NS_LNA output matching (S_{22}) from previous measurements done under several bias conditions for on-wafer and in packaged form output [6] with the new measurements on-glass. (b) One-port G-band S-parameters test setup for on-glass measurements where only 1 RF port is used.

The CPW losses have been extracted by introducing a short circuit on a dedicated substrate without die. This was done by machining the RF line to the adjacent ground using the femtosecond laser, as shown in Fig. 7.

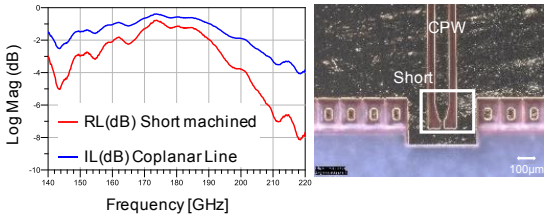

Fig. 7. Micromachined glass interposer substrate with a short circuit at the CPW line. RL (dB) measurements of the shorted structure and CPW IL calculus.

From this, it was possible to extract the CPW IL, which was calculated from measured return loss of short structure [$RL_{ShortMachined}$ (dB)] as reported in eq. (1):

$$IL_{CPW}(dB) = \left|\frac{RL_{ShortMachined}(dB)}{2}\right|. \quad (1)$$

The CPW IL have been estimated to be 2 dB in average over the G-band. One key feature is the constant output matching observed regardless of NS biasing condition, which is of utmost importance for noise measurement accuracy when using the two temperatures method, also referred as the Y factor method.

B. On-Interposer Excess Noise Ratio Extraction Methodology

1) Methodology

As developed in [4], the block diagram of the setup used to perform on- and off-wafer ENR extraction is shown in Fig. 8. The effective noise power was measured for several NS bias states and transposed to available noise power at the input plane B of the noise receiver (NRCV). From a practical standpoint, two separate noise receivers were used over the 130-170 GHz and 170-220 GHz bands, with the knowledge of their noise factor F_{RCV}, characterized in previous works with the Y-factor method [4].

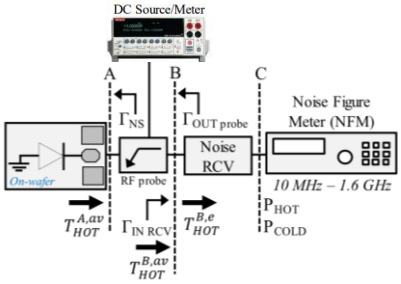

Fig. 8. Block diagram of the setup used to perform the ENR extraction at on-wafer plane (A) and off-wafer plane (B) after noise power measurements of the amplified NS were conducted at the input plane of the noise figure meter NFM (C) [4].

The first step in extracting the ENR_{av} at the input plane A of the probe, noted $ENR_{A,av}$ is to determine the noise power available at plane B from the effective noise temperature $T_{HOT}^{B,eff}$ when the diode is biased. The noise receiver temperature T_{RCV} is deduced from the measured value F_{RCV} and provides the calculation of $T_{HOT}^{B,eff}$

$$T_{RCV} = T_0(F_{RCV} - 1) \quad (2)$$

with $T_0 = 290$ K. Using the NS in low and high state, the *Y*-factor is defined as:

$$Y = \frac{P_{HOT}}{P_{COLD}} \quad (3)$$

where P_{HOT} refers to the ON-state when the diode is biased in its avalanche regime, and P_{COLD} refers to the OFF-state when the diode is unbiased. Then $T_{HOT}^{B,eff}$ of the RCV is given by the following equation:

$$T_{HOT}^{B,eff} = T_{RCV} \times (Y - 1) + Y \times \frac{T_{COLD}}{M} \quad (4)$$

where M is the impedance mismatch coefficient between the amplified NS on glass interposer and the NRCV, defined in eq. (5). T_{COLD} is the NS equivalent noise temperature when the NS and the LNA are unbiased and supposed to be as the standard temperature T_0 and the physical ambient temperature T_A.

$$M = \frac{1-\left|\Gamma_{OUT}^{probe} \times \Gamma_{IN}^{RCV}\right|^2}{\left(1-\left|\Gamma_{OUT}^{probe}\right|^2\right) \times \left(1-\left|\Gamma_{IN}^{RCV}\right|^2\right)}. \quad (5)$$

It is worth noting that the NRCV features an isolator at its input and is therefore considered as a 50Ω load. The reflection coefficient at the output of the probe is calculated in eq. (6), based on the S-parameter of the probe and the reflection coefficient of the amplified NS on the glass interposer:

$$\Gamma_{OUT}^{probe} = S_{22}^{probe} + \frac{S_{12}^{probe} S_{21}^{probe} \Gamma_{NS}}{1 - S_{11}^{probe} \Gamma_{NS}}. \quad (6)$$

Second, the available hot noise temperature is determined in eq. (7), by the use of the mismatch factor

$$T_{HOT}^{B,av} = T_{HOT}^{B,eff} \times M. \quad (7)$$

The third step corresponds to the transposition of the noise temperature at plane B to plane A. Knowing the available gain of the probe used G_{probe}^{av}, $T_{HOT}^{A,av}$ is determined in eq.(9)

$$G_{probe}^{av} = \left|S_{21}^{probe}\right|^2 \frac{(1-|\Gamma_{NS}|^2)}{\left|1-S_{11}^{probe}\Gamma_{NS}\right|^2 \times \left(1-\left|\Gamma_{OUT}^{probe}\right|^2\right)} \quad (8)$$

$$T_{HOT}^{A,av} = \frac{T_{HOT}^{B,av} - T_A\left(1 - G_{probe}^{av}\right)}{G_{probe}^{av}}. \quad (9)$$

Finally, the available $ENR_{A,av}$ at plane A can be determined by the use of the following equation:

$$ENR_{A,av}(dB) = 10\log\left(\frac{T_{HOT}^{A,av} - T_{COLD}}{T_0}\right). \quad (10)$$

2) *On-Interposer Available $ENR_{A,av}$ Extractions*

The extracted ENR_{av} values are plotted in Fig. 9 for low and high state of the NS. The results show that the ENR_{av} is monitorable, reaching levels of up to 29 dB with a 2 dB flatness within the 140-170 GHz range.

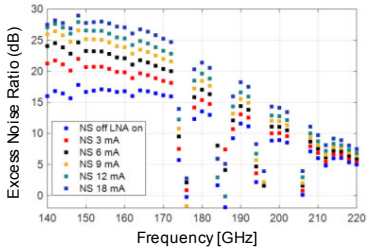

Fig. 9. Extracted ENR_{av}(dB) in G-band for the amplified NS on-glass interposer under several bias conditions.

Some ENR_{av} values are either missing or exhibit divergences, primarily attributable to the NRCV's frequency response. Specifically, the noise receiver mixer exhibits limitations in gain conversion at singular frequency points, resulting in reduced sensitivity of the noise receiver.

V. Measurements Repeatability Assessment in G-Band

A. *S-Parameters Measurement Repeatability*

One-port S-parameters measurements were performed for three different assembled NS on glass interposers in G-band. The measured S_{22} is shown in Fig. 10 with a level below -12 dB across the entire frequency band despite of the resonance observed between 170 and 180 GHz in assembly 3.

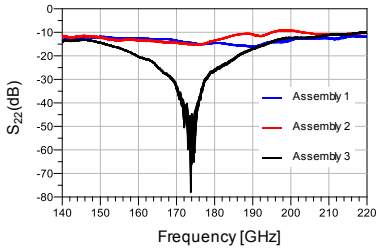

Fig. 10. S-parameters repeatability measurements in G-band of three amplified NS on glass interposer assemblies.

B. *ENR_{av} Measurement Repeatability*

An assessment of generated ENR_{av} variability for the three assembled NS chips on glass interposers was conducted in G-band. The results, depicted in Fig. 11, show a maximum ENR_{av} variability between assemblies 1 and 2 of 0.3 dB over the 140-170 GHz, where it increases up to 2 dB for assembly 3 between 162-170 GHz, confirming the impact of the resonance observed in S_{22}. It is important to mention that in Fig. 11, singular frequency points mentioned above in Fig. 9 have been removed to better represent the consistency of the ENR measurements.

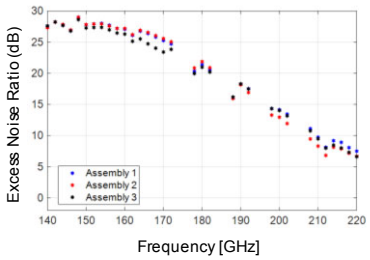

Fig. 11. ENR_{av} repeatability measurements of three amplified NS on glass interposers assemblies for high state (NS 18mA/LNA ON) in G-band. Singular frequency points observed in Fig. 9 have been excluded.

VI. Conclusion and Prospects

In this article, a new substrate technology has been developed to integrate an amplified NS based on SiGe BiCMOS technology operating in G-band. The substrate hosting the chip is an ultra-thin glass AF32 from Schott, recognized for its suitability in high frequency packaging. S-parameters and ENR_{av} have been measured in G-band and for 3 assemblies, showing a constant output matching below -12 dB in the G-band and a monitorable ENR_{av} level up to 29 dB between 140-170 GHz. The proposed substrate has considerably reduced the losses through the signal propagation path. As a prospect, it is possible to fabricate the CPW probe on the same substrate to be coupled with the NS to perform on-wafer noise measurements in G-band.

Acknowledgment

This work was supported by the STMicroelectronics-IEMN joint Laboratory, the French government through the National Research Agency (ANR) under program PIA EQUIPEX LEAF ANR-11-EQPX-0025, and the French RENATECH network on micro and nanotechnologies.

References

[1] P. Chevalier et al, "SiGe BiCMOS Current Status and Future Trends in Europe", 2018 IEEE BiCMOS Compd. Semicond. Integr. Circuits Technol. Symp. BCICTS, pp. 64–71, 2018

[2] J.C Goncalves et al, "A 130 to 170 GHz integrated noise source based on avalanche silicon Schottky diode in BiCMOS 55 nm for in-situ noise characterization", International Conference of Microelectronic Test Structures (ICMTS), pp. 1-3, 2017.

[3] S. Bouvot et al, "A 140 GHz to 160 GHz active impedance tuner for in-situ noise characterization in BiCMOS 55 nm", IEEE International Symposium on Radio-Frequency Integration Technology (RFIT), pp. 153-155, 2017.

[4] J. C. Goncalves et al., "Millimeter-wave noise source development on SiGe BiCMOS 55-nm technology for applications up to 260 GHz", IEEE Trans. Microw. Theory Techn., vol. 67, no. 9, pp. 3732–3742, 2019.

[5] V. Fiorese et al, "A 140 GHz to 170 GHz Active Tunable Noise Source Development in SiGe BiCMOS 55 nm Technology", 16th European Microwave Integrated Circuits Conference (EuMIC), pp. 125-128, 2021

[6] V. Fiorese, "Nano sonde active intelligente pour mesures de bruit et de puissance dans la bande de fréquence 130-260 GHz", These de doctorat, Université de Lille, 2022.

[7] V. Fiorese et al, "A G-band Packaged Amplified Noise Source Using SiGe BiCMOS 55 nm Technology", IEEE Transactions on Microwave Theory and Techniques, pp. 1-15, 2023.

[8] V. Fiorese, "220 GHz E-Plane Transition from Waveguide to Suspended Stripline Integrated on Industrial Organic Laminate Substrate Technology", 51st European Microwave Conference (EuMC), pp. 99-102, 2021.

[9] L. Zhang et al, "Development of SnAg-based lead free solders in electronics packaging", Microelectronics Reliability, pp. 559-578, 2012.